Electronic Supplementary Material (ESI) for Nanoscale.

Redox-Switchable Host-Guest Complexes of Metallocenes and [8]Cycloparaphenylene

Hyejin Kwon,[a], Brian Newell[b] and Carson J. Bruns[ac*]

[a]*Department of Mechanical Engineering, University of Colorado, Boulder, 427 UCB, 1111 Engineering Drive, Boulder, CO 80309.*
[b]*Materials and Molecular Analysis Center, Analytical Resources Core, Colorado State University, 200 W. Lake Street, Fort Collins, CO 80523*
[c]*ATLAS Institute, 1125 18th St. 320 UCB, Boulder, CO 80309*

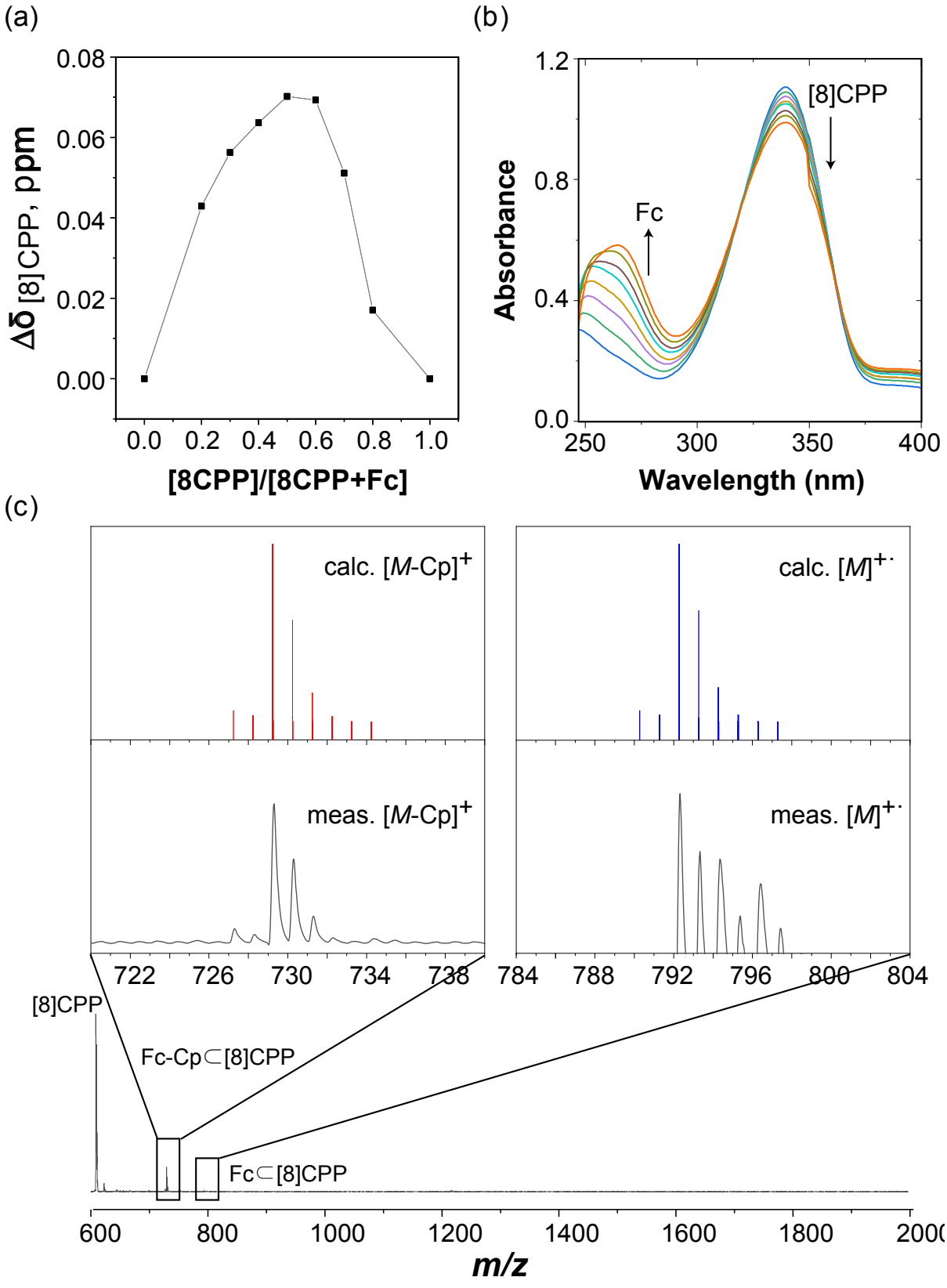

Fig. S 1 Fc⊂[8]CPP characterization data. (a) Job plot. The chemical shift of [8]CPP (^{1}H NMR, 300 MHz, $CDCl_3$) was plotted as a function of molar fraction, [8CPP]/[8CPP+Fc]. (b) Ultraviolet absorption spectra of [8]CPP (5.5×10^{-4} M in chloroform) with increasing Fc concentration (1:0 to 1:1.2 [8]CPP:Fc). Isosbestic points are observed at 320 and 365 nm. (c) MALDI-TOF-MS of Fc⊂[8]CPP shows signals for $[M–Cp]^+$ and $[M]^{+\cdot}$.

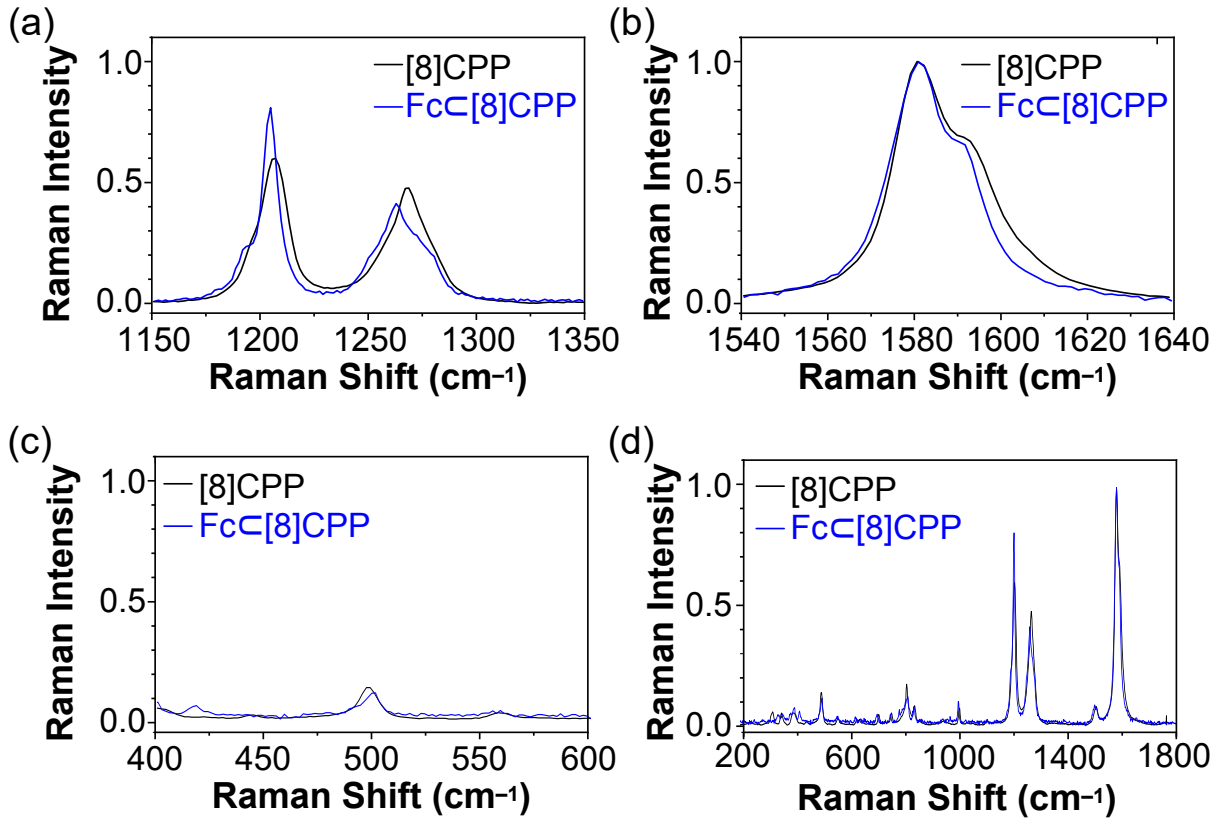

Fig. S 2 Raman spectra comparing [8]CPP and a 1:1 of Fc:[8]CPP mixture. (a) inter-,intrabenzene C-H bending (b) C-C stretching, (c) low energy vibration, and (d) full spectra. 532 nm laser excitations were used.

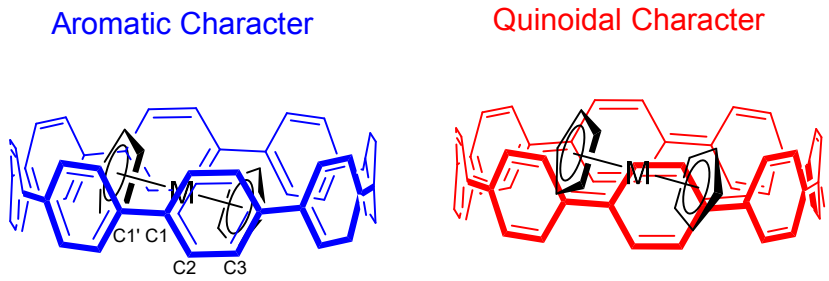

	C1-C1´	C1-C2	C2-C3	ΔI
[8]CPP	1.486	1.401	1.383	-0.019
Fc⊂[8]CPP	1.494	1.395	1.380	-0.015
	1.484	1.395	1.381	-0.014
$CoCp_2^+$⊂[8]CPP	1.482	1.397	1.383	-0.014
	1.534	1.362	1.433	0.071

Increasing Aromatic Character ↓

Fig. S 3 Comparing bond lengths in the solid-state structures of [8]CPP, Fc⊂[8]CPP, and $CoCp_2^+$⊂[8]CPP. The ΔI is the difference between C2-C3 and C1-C2. The solid-state structures were obtained from single crystal X-ray Diffraction.

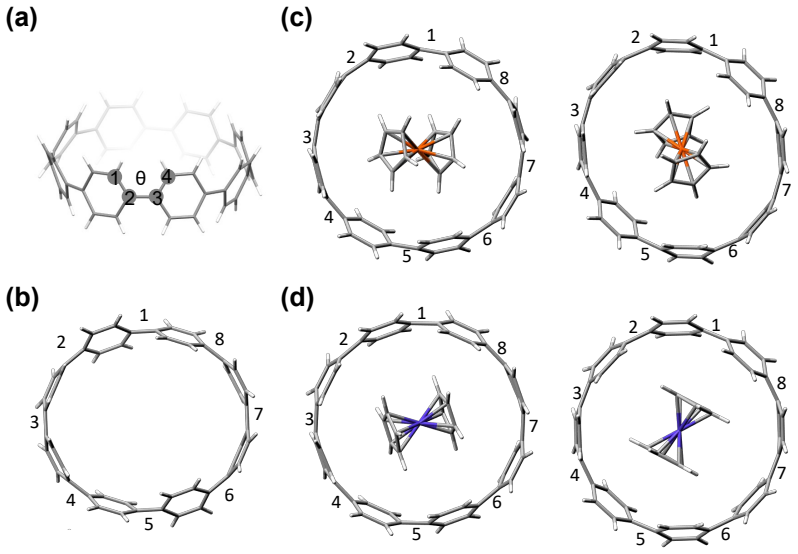

Dihedral angle, θ	[8]CPP (°)	Fc⊂[8]CPP (°)		$CoCp_2^+$⊂[8]CPP (°)	
1	33.9	36.1	39.7	27.3	30.2
2	-22.7	-20.2	-24.3	-14.8	-26.3
3	2.3	-1.7	-1.9	-3.9	6.2
4	26.4	29.1	24.5	22.1	23.5
5	-40.4	-35.3	-34.8	-26.1	-32.1
6	19.7	18.9	26.9	16.6	27.4
7	8.5	3.6	-9.1	6.1	-5.8
8	-28.0	-31.6	-18.3	-27.1	-21.7
Avg	-0.1	-0.1	0.3	0.0	0.2
Stdev.	27.3	27.2	27.0	21.4	25.3

Fig. S 4 Comparison of dihedral angles (θ, (a)) in the single-crystal structures of (b) [8]CPP, (c) Fc⊂[8]CPP, and (d) $CoCp_2^+$⊂[8]CPP.

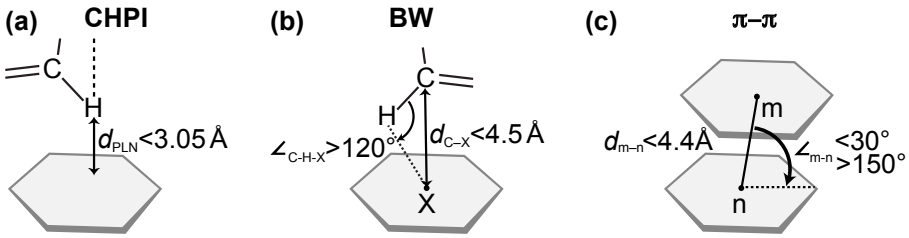

Fig. S 5 Graphical depictions of the paramaters that constrain CH–π bond according to (a) the CHPI program and (b) the Brandl-Weiss (BW) method, as well as the geometric cut-offs for (c) the π-π interaction.

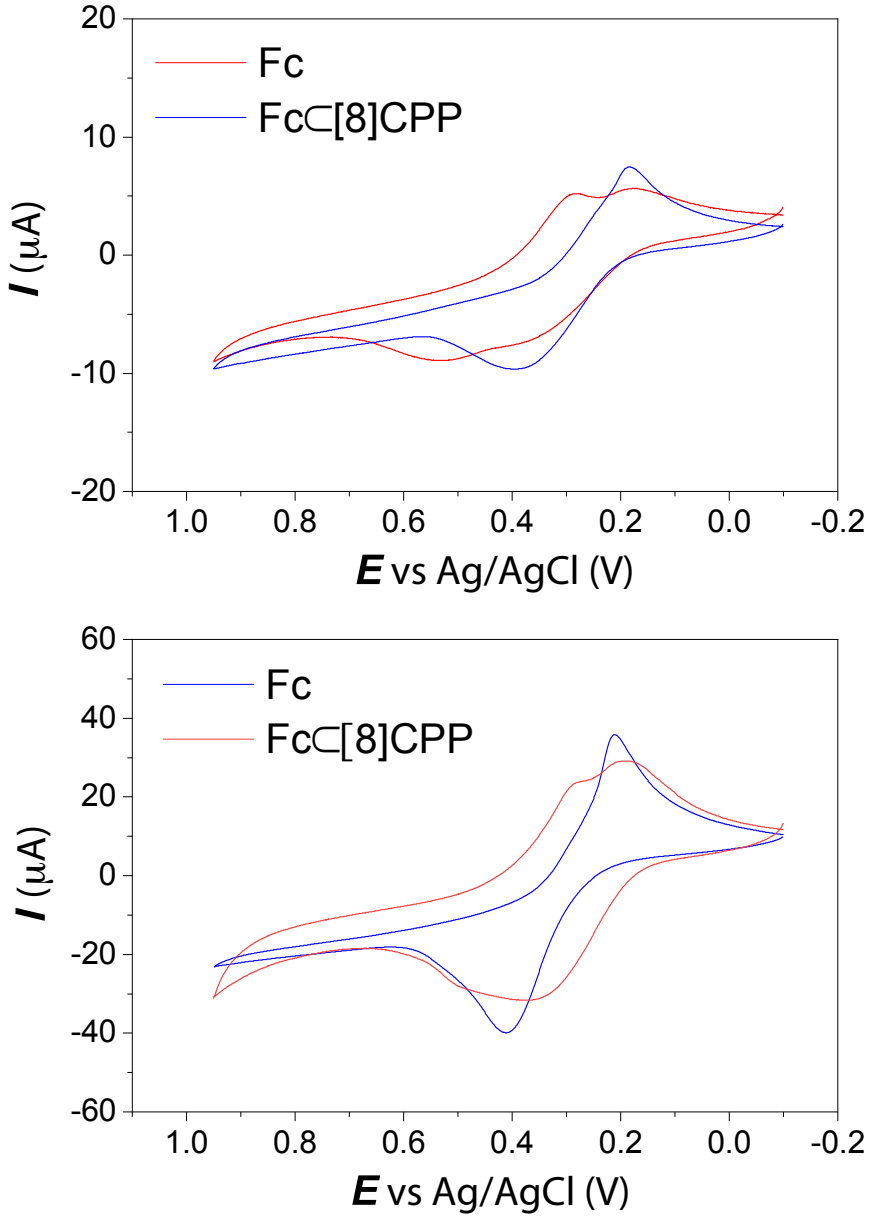

Fig. S 6 Free Fc (blue) and Fc⊂[8]CPP complex (red) on a Pt electrode in 0.3M NaCl were measured at (a) 100 mV/s and (b) 200 mV/s of CV scan rate.

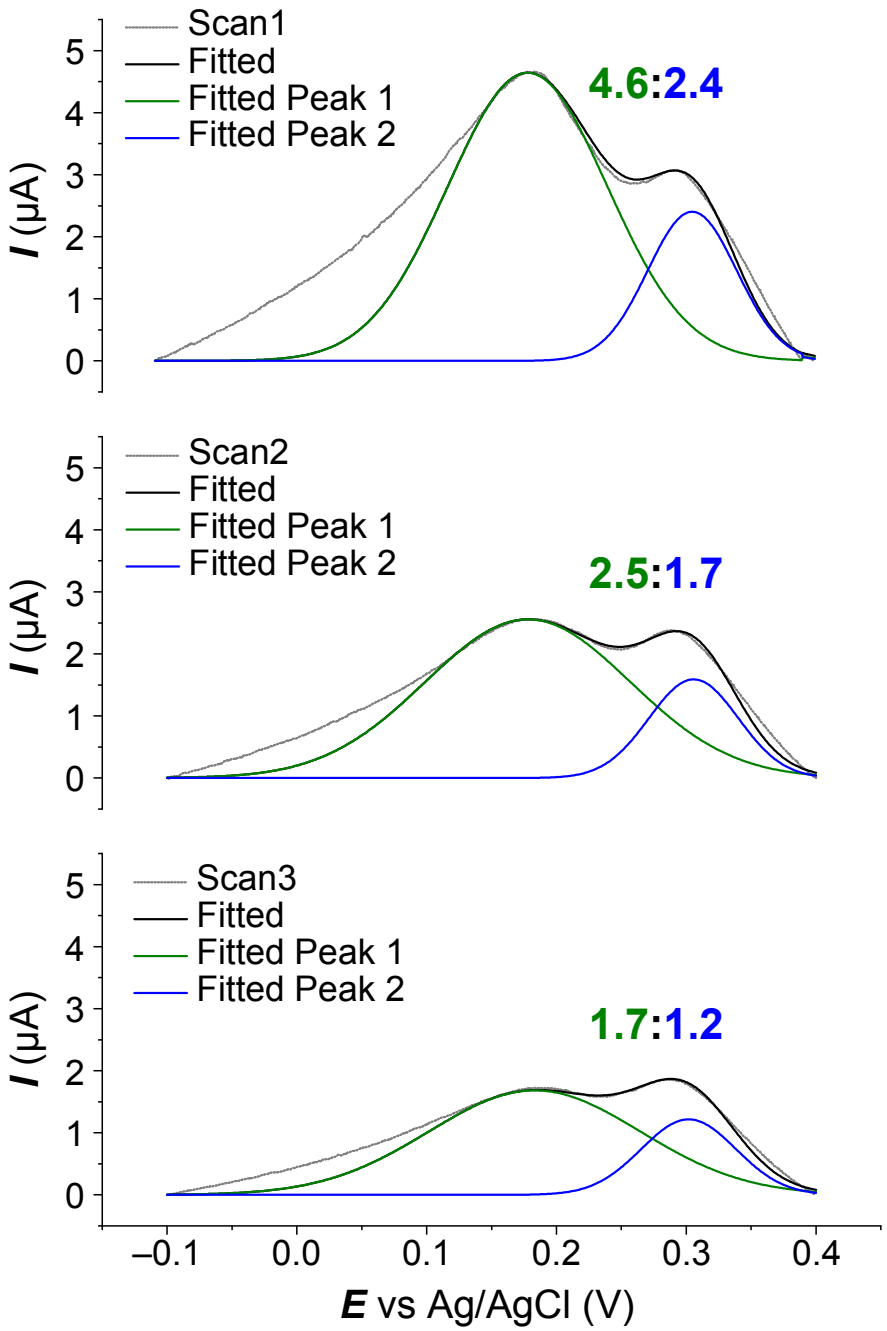

Fig. S 7 Peak fitting of three consecutive CV scans (50 mV/s, 0.3 M NaCl) of a Fc:[8]CPP mixture drop cast on a Pt electrode. The ratio of amplitudes for each fitted signal are indicated on each scan. The signal attributable to free Fc (green fitted peak) is depleted more rapidly than the signal attributable to Fc⊂[8]CPP (blue fitted peak) with each scan. Peak fitting was performed in Peakfit software. Ratios depict the relative amplitudes of each signal.

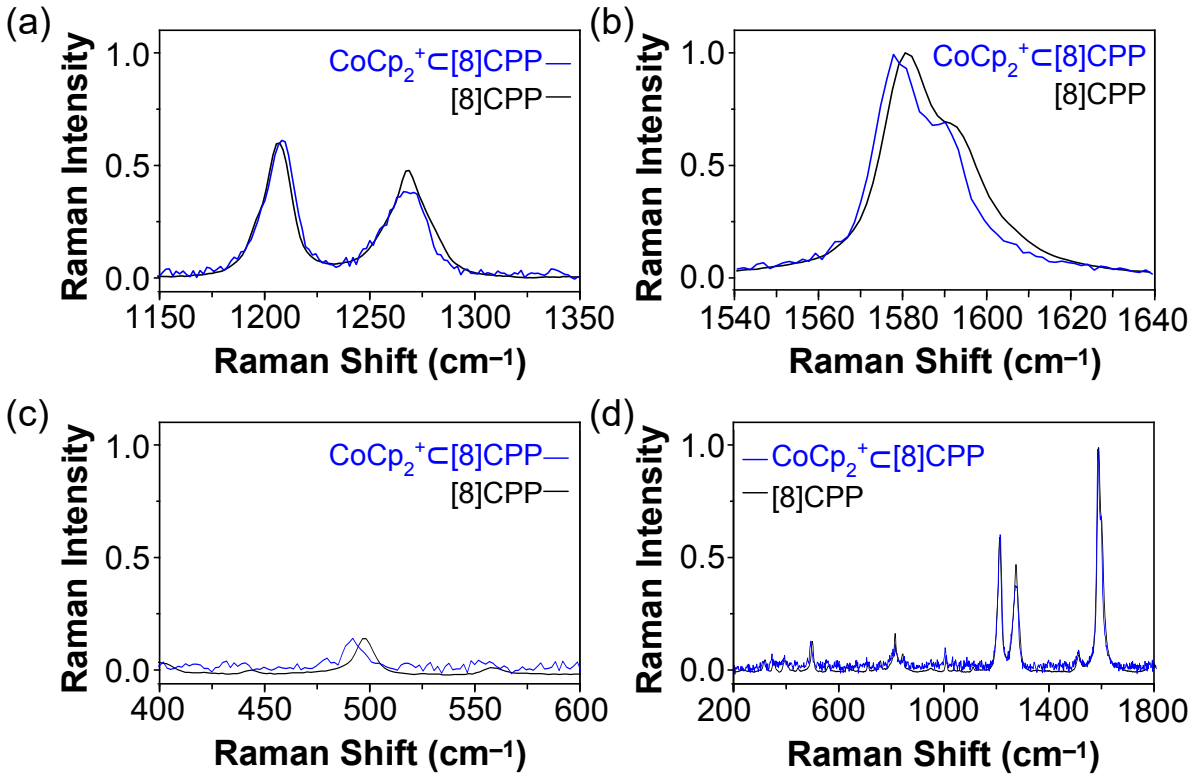

Fig. S 8 Raman spectra comparing [8]CPP and a 1:1 of $CoCp_2$:[8]CPP mixture. (a) inter-,intrabenzene C-H bending (b) C-C stretching, (c) low energy vibration, and (d) full spectra. 532 nm laser excitations were used.

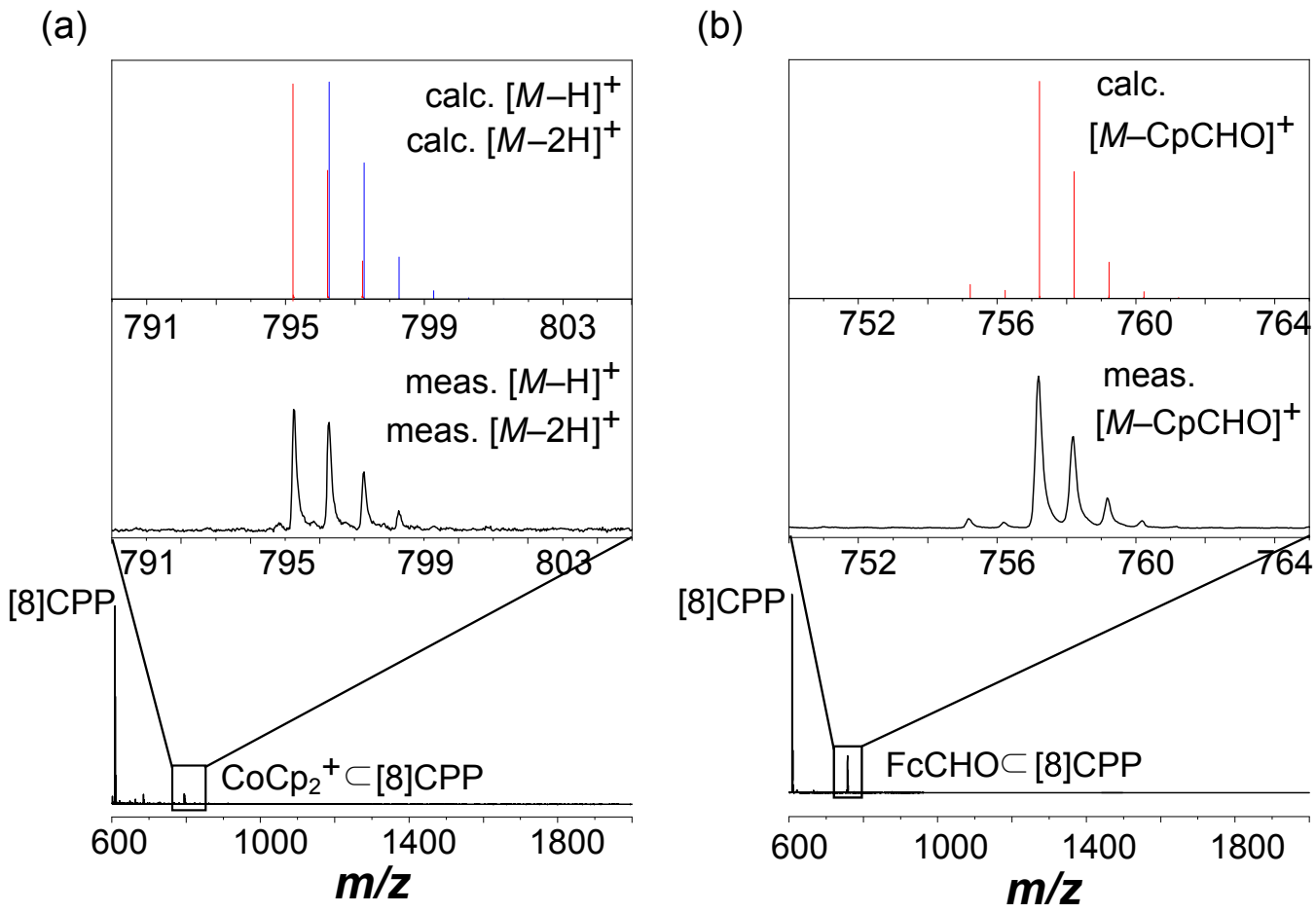

Fig. S 9 MALDI Data of (a) $Fc(CHO)_2 \subset$[8]CPP. (b) $CoCp_2^+ \subset$[8]CPP.

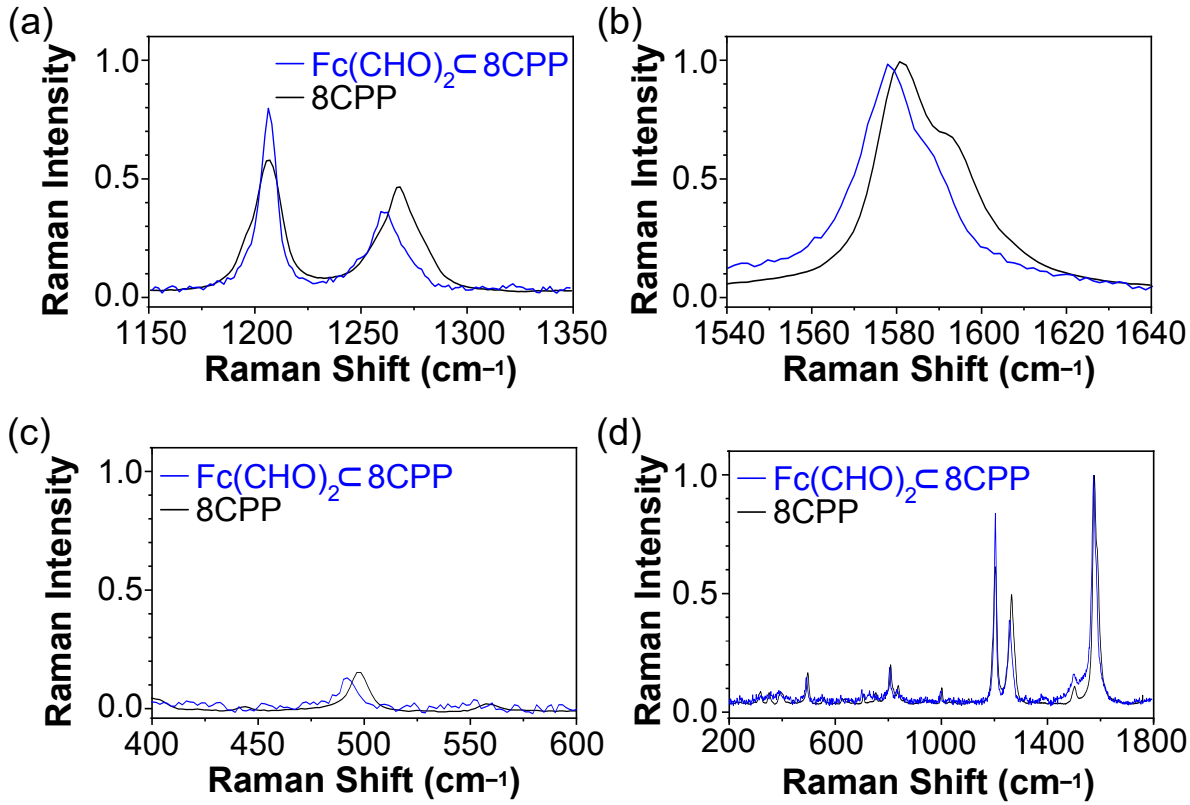

Fig. S 10 Raman spectra comparing [8]CPP and a 1:1 of $Fc(CHO)_2$:[8]CPP mixture. (a) inter-,intrabenzene C-H bending (b) C-C stretching, (c) low energy vibration, and (d) full spectra. 532 nm laser excitations were used.

	Compound	E(Hartree)	ΔE(kcal/mol)
	8CPP	-1842.9553	
1	Fc(CHO)2-trans-uu	-1875.5505	
2	Fc(CHO)2-trans-ud	-1875.5506	
3	Fc(CHO)2-cis-uu	-1875.5504	
4	Fc(CHO)2-cis-ud	**-1875.5509**	
5	Fc(CHO)2-trans-uu⊂8CPP	-3718.5333	-17.0
6	Fc(CHO)2-trans-ud⊂8CPP	**-3718.5365**	**-19.0**
7	Fc(CHO)2-cis-uu⊂8CPP	-3718.5335	-17.1
8	Fc(CHO)2-cis-ud⊂8CPP	-3718.5287	-14.1

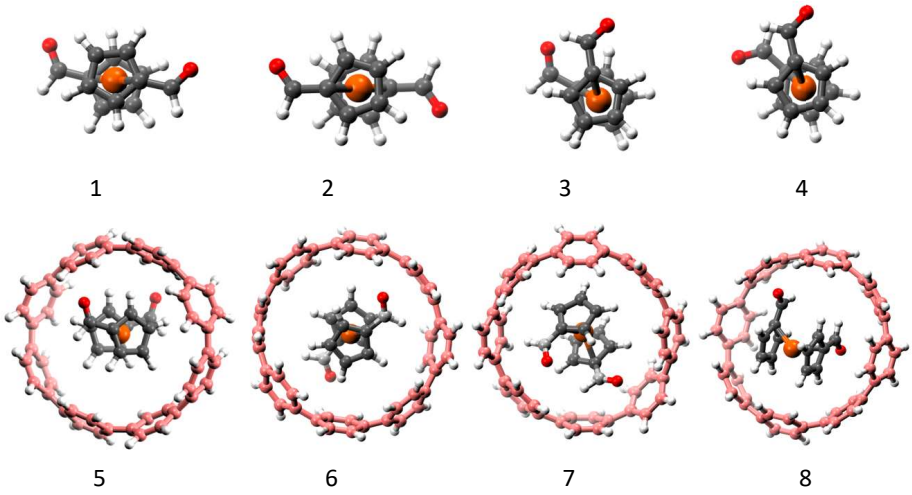

Fig. S 11 DFT calculations of *cis* and *trans* guests and complexes.ΔE is the association energy. In the case of guest molecules, most conformation has comparable energy. However, the trans confirmation has lower energy when it is complexed due to additional hydrogen bonding between oxygen in a guest molecule and hydrogen in a host molecule. u (up) and d (down) indicate two oxygen positions in Fc.

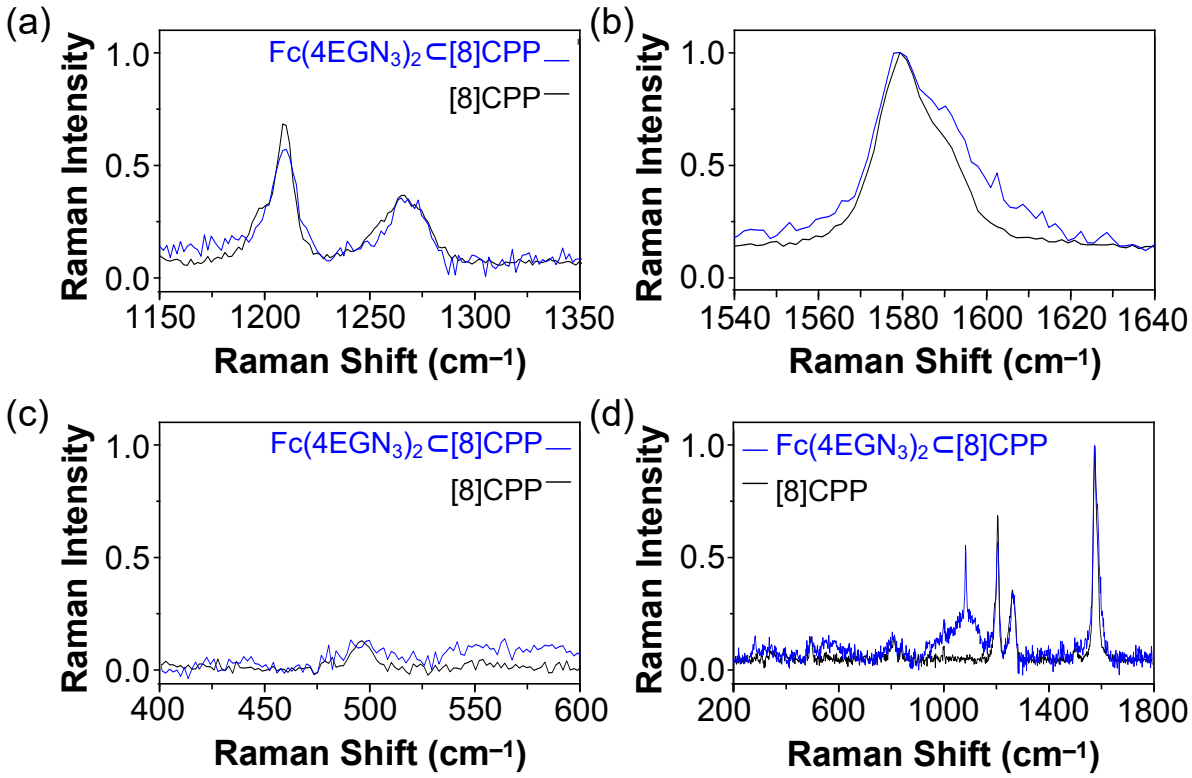

Fig. S 12 Raman spectra comparing [8]CPP and a 1:1 of $Fc(4EGN_3)_2$:[8]CPP mixture. (a) inter-,intrabenzene C-H bending (b) C-C stretching, (c) low energy vibration, and (d) full spectra. 532 nm laser excitations were used.

	Fc⊂[8]CPP	$[CoCp_2][(PF_6)]$⊂[8]CPP
CCDC Number	2150627	2150629
Empirical formula	$C_{178}H_{130}Cl_{12}Fe_3$	$C_{58}H_{42}CoF_{12}P_2$
FW (g/mol)	2861.76	1087.79
Temperature (K)	142	250
Wavelength (Å)	0.71073	0.71073
Crystal system	Monoclinic	Monoclinic
Space group	$P2_1/c$	C2/c
a (Å)	13.9205(5)	38.1212(11)
b (Å)	726.8345(9)	13.7764(4)
c (Å)	18.8544(7)	24.9606(7)
β (°)	97.032(2)	129.152(1)
Volume ($Å^3$)	6990.0(4)	10165.4(5)
Z	2	8
Density(mg/m^3)	1.360	1.422
Abs. Coeff. (mm^{-1})	0.593	0.483
F(000)	2960	4440
Crystal size (mm^3)	0.132 × 0.092 × 0.023	0.271 × 0.196 × 0.170
N_{ref}	7309	9999
GOF on F^2	1.087	2.238
Completeness	99.9%	100.00 %
R [I>2σ(I)]: R_1[a] (wR_2[b])	0.0847(0.2231)	0.1332 (0.4156)
R indices (all data) R_1[a] (wR_2[b])	0.1274(0.2591)	0.1475 (0.4512)

a) $R_1 = \Sigma||F_o| - |F_c||/\Sigma|F_o|$, b) $wR_2 = [\Sigma[w(F_o^2-F_c^2)^2]/\Sigma[w(F_o^2)^2]]^{½}$, $w = 1/[\ ^2(F_o^2) + (aP)^2 + bP]$, where $P = [\max(F_o^2 \text{ or } 0) + 2(F_c^2)]/3$

Table S 1 XRD Data for Fc⊂[8]CPP and $CoCp_2PF_6$⊂[8]CPP.